Energy Engineering

Tech Science Press

Doi:10.32604/ee.2025.074440

ARTICLE

Microgrid Scheduling with the Participation of Electric Vehicles under Extreme Weather Conditions

Zujun Ding, Zhi Liu, Peng Huang, Yuhan Qian, Chengyi Li, Zizhuo Yu, Hui Huang, Baolian Liu, Wan Chen and Jie Ji*

Electric Engineering Department, Huaiyin Institute of Technology, Huaiyin, China

*Corresponding Author: Jie Ji. Email: jijie@hyit.edu.cn

Received: 11 October 2025; Accepted: 27 November 2025; Published: 27 May 2026

ABSTRACT: Under extreme weather conditions (such as hurricanes and heatwaves causing sudden drops in renewable energy output and surges in load), microgrid operations face severe challenges due to the uncertainty of renewable energy and load fluctuations. Although existing research has focused on microgrid optimal scheduling or electric vehicle integration, there has not yet been a systematic approach to multi-timescale scheduling that combines electric vehicle fleets under extreme weather scenarios, and particularly, explicit modeling of weather events and their impact on component failure rates and transmission lines is lacking. This paper proposes, for the first time, a multi-timescale optimal scheduling strategy integrated with an electric vehicle fleet, filling this gap. By constructing a microgrid model containing diesel generators, micro gas turbines, renewable energy sources, energy storage, and demand response loads, and defining four typical extreme weather scenarios (high solar & high wind, high solar & low wind, low solar & high wind, low solar & low wind) to simulate the impact of extreme events, a day-ahead and intraday coordinated framework aiming to minimize total operating costs is established. In this framework, the day-ahead stage formulates a preliminary plan based on wind and solar forecasts, while the intraday stage employs the mobile energy storage characteristics of the electric vehicle fleet for rolling adjustments to cope with renewable fluctuations and sudden load changes. Simulations based on actual data from Huai'an City in 2024 show that this strategy can significantly reduce microgrid operating costs (by 5.6%–7.2%), increase renewable energy utilization (94%–96%), reduce carbon emissions (17.8%–22.6%), and enhance the system's economic performance and resilience under extreme weather conditions.

KEYWORDS: Microgrid; electric vehicle cluster; multi-time scale scheduling; extreme weather; renewable energy absorption; optimal operation; demand response

1 Introduction

As the proportion of renewable energy in the energy structure continues to increase, distributed power generation systems [1,2] have effectively reduced transmission and distribution losses by taking advantage of the local consumption feature. Clean energy sources such as wind power and photovoltaic power [3,4] are increasingly replacing traditional fossil fuels, and their economic and ecological benefits are gradually emerging. However, due to the influence of extreme weather [5,6], a large number of uncontrollable distributed power sources are connected to the grid, especially the strong volatility characteristic of wind and solar power generation [7,8], which poses severe challenges to the security and stability of the power system.

Under the continuous penetration of the concept of energy internet, the coordinated optimization development form of multi-energy complementary microgrids that integrate wind, solar, and thermal storage

has become an important way to solve the effective utilization of distributed renewable energy. Currently, many scholars have conducted in-depth research on the optimal scheduling of microgrids. The optimal scheduling of microgrids must consider factors such as the output of renewable energy, load absorption, and the operating status of system components, such as the uncertainty and volatility of energy output from wind and solar energy, which have certain impacts on the scheduling of controllable units and energy storage capacity within the microgrid. Reference [9] proposed an optimal scheduling method for a microgrid based on model predictive control (MPC) and CHP, while References [10,11] established a day-ahead and real-time scheduling model for microgrids and proposed a two-stage stochastic programming model to handle the uncertainty of photovoltaic and wind power. References [12,13] introduced a carbon trading mechanism into the scheduling model to achieve multi-objective optimization of economic and environmental benefits. Most of these studies focused on the optimal scheduling within traditional microgrids. Currently, there is continuous development and a tendency towards large-scale integration of electric vehicle charging stations into microgrids, which, to a certain extent, has changed the energy optimization configuration pattern within the microgrid. Electric vehicles [14], as a form of clean energy, through the effective aggregation of battery characteristics, the large-scale and clustered battery energy storage capacity of electric vehicles, combined with reasonable scheduling, can not only alleviate the intermittent and uncertain impacts of renewable energy such as wind and solar power, but also provide frequency regulation and peak shaving [15–17] and other auxiliary services for the power grid to a certain extent.

As flexible energy storage resources on the demand side, the participation of clustered electric vehicles in the optimal scheduling of microgrids can further improve the operational reliability of the system. Many scholars have conducted research on the operation optimization scheduling of integrated energy systems with electric vehicles in microgrids. Reference [18] proposed an EV charging and discharging strategy based on dynamic electricity prices to optimize the real-time energy balance and economy of the microgrid. Reference [19] proposed a dynamic time-of-use charging price setting strategy considering user satisfaction, constructed an electric vehicle grid connection scenario, and predicted its controllable capacity. Reference [20] proposed a two-layer charging and discharging scheduling model for electric vehicles considering user satisfaction for the energy scheduling problem of large-scale random access of electric vehicles to the grid, but none of these references considered the multi-time-scale analysis of the economic scheduling of electric vehicle clusters participating in a microgrid under extreme weather conditions.

This paper proposes a multi-time-scale optimization scheduling strategy for microgrids integrating electric vehicle clusters to address the uncertainty of wind and solar power output under extreme weather conditions and the scheduling problem of interruptible and transferable loads based on load importance. Firstly, the study modeled the controllable energy storage, various loads (including interruptible and transferable loads), diesel generators, and micro gas turbine units as key components in the microgrid system, and incorporated equipment operation and maintenance costs, economic compensation costs, carbon emission costs, and the overall revenue of the microgrid into the comprehensive optimization objective. On this basis, a multi-time-scale energy management framework was constructed. This framework established a day-ahead operation optimization scheduling model and an intraday operation optimization scheduling model that included the participation of electric vehicle clusters. In the current stage, the initial plan is mainly formulated based on predictive information, while in the intraday stage, it is continuously optimized and adjusted based on real-time data to cope with the fluctuations of renewable energy and load. Finally, to verify the effectiveness of the proposed method, the study used the typical microgrid operation data of Huai'an City in 2024 as a case, and built a simulation model in the MATLAB environment for testing. Through detailed case analysis, the results show that this strategy can effectively improve the economic operation level and scheduling reliability of the microgrid in extreme weather scenarios.

2 Microgrid Model

This paper addresses the resilience optimization problem of multi-energy microgrids under extreme weather conditions, and constructs a collaborative scheduling framework that incorporates a high-elasticity electric vehicle cluster. The system integrates diesel generators, micro gas turbines (CHP), renewable energy sources such as wind and solar, and a composite energy storage unit. Additionally, it innovatively introduces a large-scale electric vehicle cluster with bidirectional charging and discharging capabilities as a mobile energy storage node. Through multi-energy flow coupling modeling and equipment operation constraint analysis, a stochastic optimization model for the temporal and spatial correlation of extreme weather and power load is established. The focus is on solving scenarios where the output of wind and solar power drops sharply and emergency loads surge, by leveraging the temporal shift characteristics of the state of charge (SOC) of the electric vehicle cluster and the coordinated regulation of gas turbines for thermal power generation, to achieve optimal power balance and energy supply cost. This research breaks through the traditional "source-load" one-way scheduling mode of microgrids. Through the distributed energy storage aggregation of the electric vehicle cluster and demand-side response strategies, an energy resilient supply network under disaster conditions is formed, significantly enhancing the microgrid's resilience to disasters and the efficiency of renewable energy consumption. The system architecture of the studied microgrid group is shown in Fig. 1.

2.1 Optimization Operation of Microgrid

The microgrid achieves optimized operation through the regulation of electric vehicle loads and the coordinated control of multiple devices. In the daily scheduling, economic performance is the primary goal, and the time-of-use pricing (TOU) mechanism is used to smooth out peak loads and fill in low peaks. During the day, the peak electricity demand and the charging demand of electric vehicles overlap, increasing the burden on the power grid. The microgrid scheduling system guides electric vehicles to charge at low electricity prices at night, reducing the cost for the owners and alleviating the pressure on the power grid. At the same time, as an energy storage unit, electric vehicles can release energy to support the microgrid during high power grid load and high electricity prices, reducing the burden on the power grid. At night, the charging demand of electric vehicles may overlap with the peak electricity demand of residents. The microgrid scheduling system needs to comprehensively consider and formulate the optimal charging plan to ensure the satisfaction of charging demands, reduce the impact on other devices, and utilize low electricity price periods for charging, thereby reducing the overall cost.

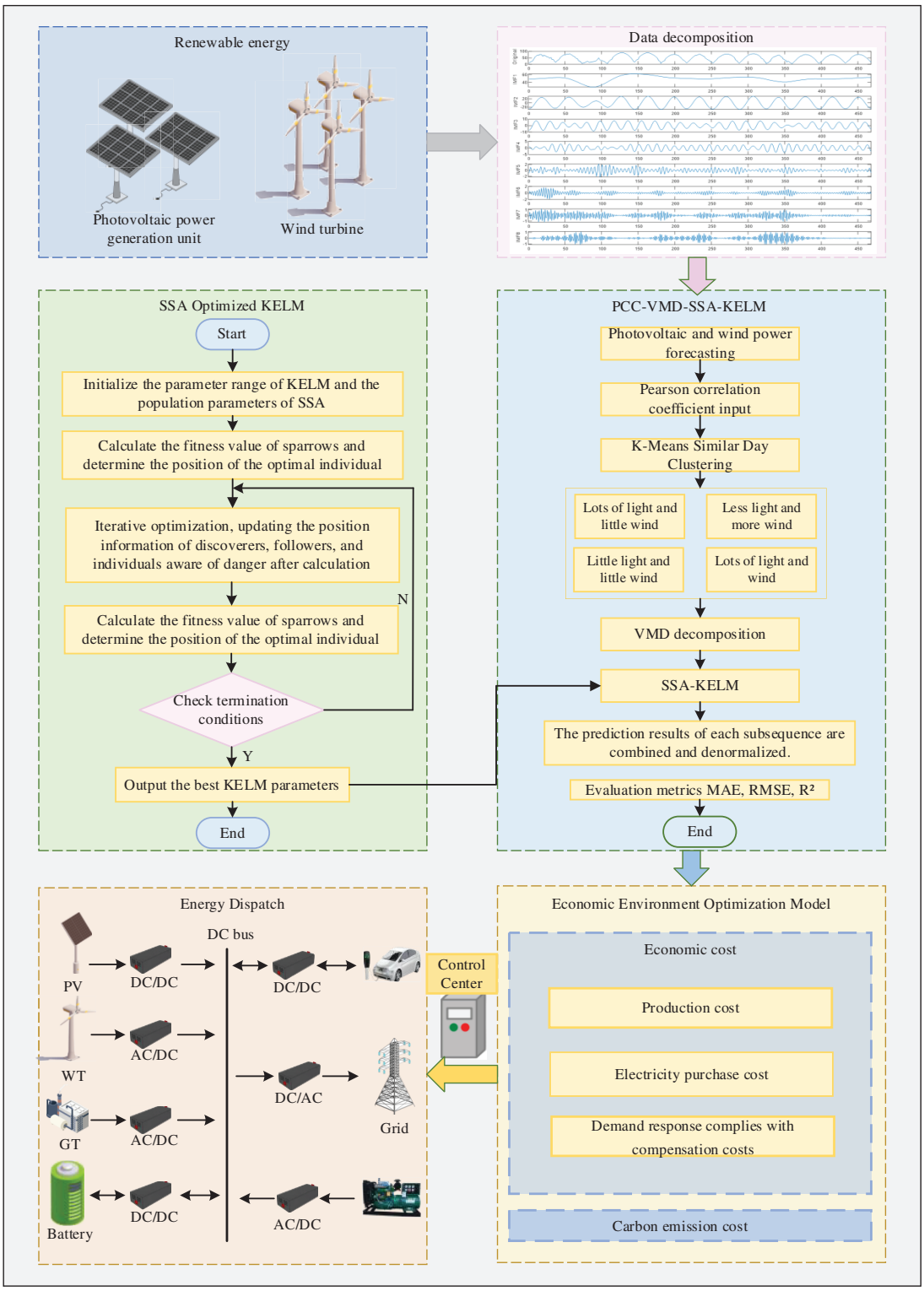

Figure 1: Microgrid cluster system architecture

2.2 Microgrid Multi-Time Scale Energy Optimization Scheduling Considering the Impact of Extreme Weather on Electric Vehicle Participation

With the integration of distributed generation, especially the high proportion of renewable energy access, the integration of green energy, such as wind power and photovoltaics, their output has uncertainty, uncontrollability and unpredictability, which will inevitably have many impacts on the power grid. Large-scale integration will increase the accommodation problems of the power system and may lead to wind and solar power outages. At the same time, the impact of extreme weather on new energy generation and power grid operation cannot be ignored. Studies have shown that the impact of extreme weather intensifies the risks of equipment failures and system instability, and the high proportion of new energy access in the new power system further amplifies the impact of fault propagation. Wind power and photovoltaic power are highly susceptible to extreme weather and may experience large-scale shutdowns and output losses. In severe cases, they may threaten the safe and stable operation of the power grid. Based on these reasons, this paper integrates distributed power sources into the microgrid to achieve coordinated and optimized control of various devices within the microgrid, reducing the impact on the external power grid. Through multi-time scale coordinated optimization scheduling of the day-ahead plan and the adjustment of daily operation, the randomness of renewable energy within the microgrid is reduced externally on the power grid. In the day-ahead stage, the energy output of wind and solar power for the next day is predicted. When the real-time operation deviates from the day-ahead prediction within the day, the scheduling plan can be flexibly adjusted. In the daily optimization scheduling stage, by utilizing the idle storage capacity of clustered electric vehicles, the day-ahead optimized scheduling is corrected. When the system energy scheduling deviates due to uncontrollable output factors such as wind power and photovoltaic power, resource allocation based on idle storage capacity of electric vehicles during off-peak electricity prices is carried out to achieve peak shaving and valley filling, improving the absorption of new energy, effectively reducing the capacity configuration of the internal energy storage system, and greatly reducing the construction cost of the system. The multi-time scale optimization scheduling framework of the studied microgrid is shown in Fig. 2.

3 A Multi-Time-Scale Optimization Model for Microgrids Considering the Randomness of Extreme Weather

3.1 The Day-Ahead Scheduling Model for Microgrids Considering the Randomness of Extreme Weather

The constraints of the day-ahead scheduling model include battery energy storage, load demand, diesel generators, micro gas turbines, photovoltaic generators, and wind power generators, as shown in the following equation:

(1) Battery energy storage

The operation constraints of the battery, as the energy storage device of this micro-energy network, mainly include power constraints and state-of-charge constraints:

$$\begin{cases} 0 \le P_{ESS,t}^{ch} \le P_{ESS,t,\max}^{ch} \cdot u_{ch.t} \\ 0 \le P_{ESS,t}^{dis} \le P_{ESS,t,\max}^{dis} \cdot u_{dis,t} \\ u_{ch.t} + u_{dis,t} \le 1 \end{cases} \tag{1}$$

$$\begin{cases} SOC^{\min} \le SOC(t) \le SOC^{\max} \\ SOC(t+1) = SOC(t) + \eta_{ch} \cdot \frac{P_{ESS,t}^{ch} \Delta t}{E_{\text{rated}}} - \frac{P_{ESS,t}^{dis} \Delta t}{\eta_{dis} \cdot E_{\text{rated}}} \end{cases} \tag{2}$$

where $P_{ESS,t}^{ch}$ and $P_{ESS,t}^{dis}$ represent the charging and discharging power at time t, respectively; $P_{ESS,t,\max}^{ch}$ and $P_{ESS,t,\max}^{dis}$ are the maximum charging and discharging power limits of the battery; $u_{ch.t}$ and $u_{dis,t} \in (0,1)$ are

the charging and discharging status indicator variables, ensuring mutual exclusivity; $SOC\,(t)$ is the state of charge at time t; η_{ch} and η_{dis} are the charging and discharging efficiencies, respectively; E_{rated} is the rated capacity of the battery; Δt is the time interval.

The operating cost F_{BC} of battery energy storage is:

$$F_{\text{BC}} = \sum_{i \in M} \left(b_{i,t} f_{\text{dis}} \eta_{e,i,t} + f_{\text{cycle}} \right) \tag{3}$$

where M represents the set of energy storage devices; $b_{i,t}$ indicates the charging and discharging status of energy storage device i at time t; $b_{i,t} = 1$ represents that the energy storage is in a charging state; $b_{i,t} = 0$ represents that the energy storage is in a discharging state; f_{dis} is the maintenance cost for charging and discharging; $\eta_{e,i,t}$ is the charging and discharging power of energy storage device i at time t; f_{cycle} is the cost corresponding to the wear and tear of the energy storage device.

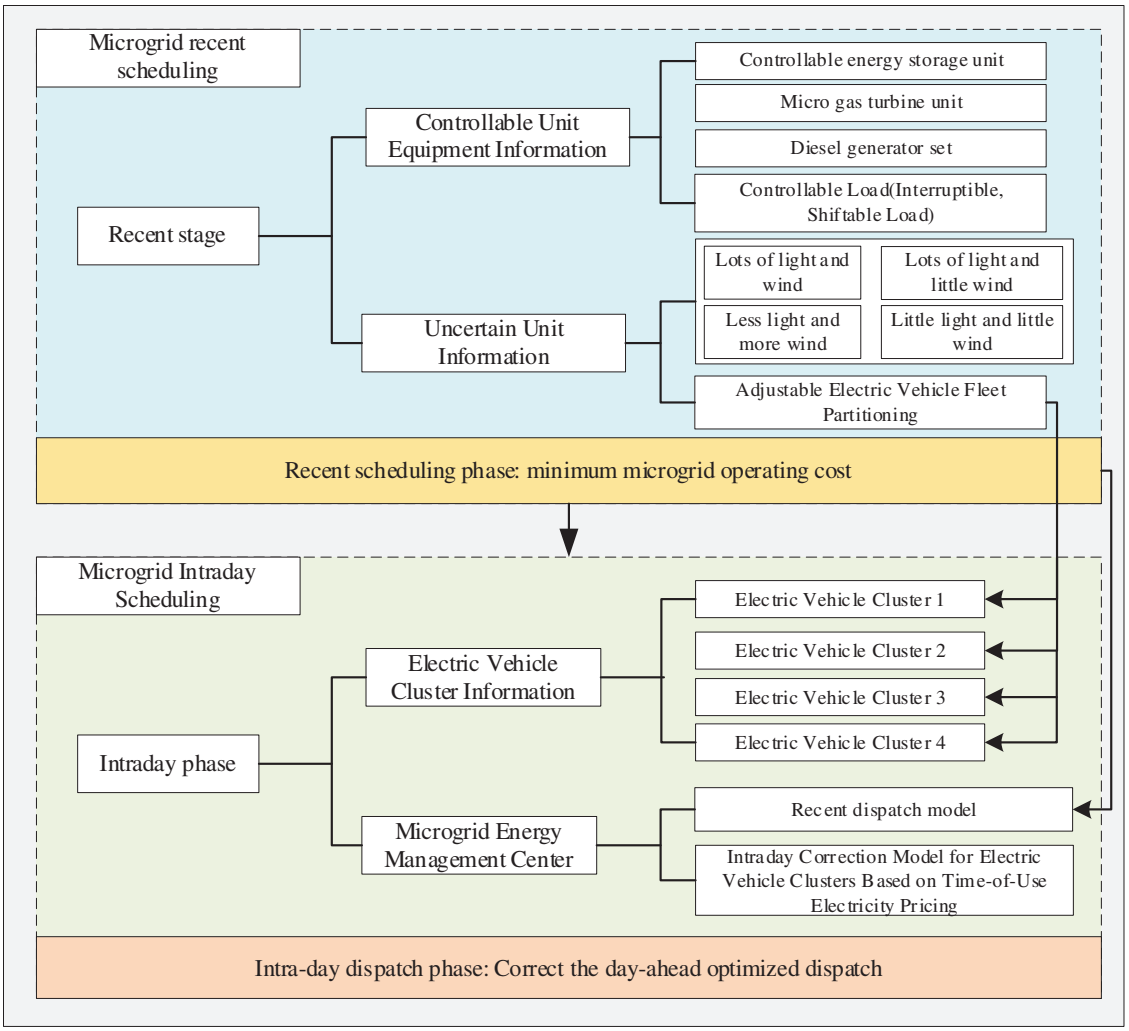

Figure 2: Multi-time-scale optimization scheduling framework for microgrid

(2) Load demand

The demand response load model within the microgrid includes interruptible loads and transferable loads. When the microgrid is in a peak load period or when the operational reliability is slightly threatened, the commonly used adjustment method is to provide some economic compensation to power users, expecting to reduce or even interrupt some certain electricity loads. This part of the load is called interruptible load, and the prerequisite is that an agreement needs to be signed between the operator and the user. The user is promised to receive compensation fees when the load is interrupted. Different levels of load are associated with different compensation fee ratios in the agreement. Similarly, transferable loads refer to the introduction of transferable loads to participate in the regulation during the period when the microgrid needs to allocate resources. For example, household appliances of residents, such as air conditioners. The same as the handling of interruptible loads, corresponding compensation fees are paid to the users participating in the regulation, guiding users to shift more to the low-load period for electricity consumption. Demand response loads can increase the reserve rate of the microgrid, reduce the purchase volume from the distribution network, and improve the economic and reliability performance of the microgrid operation.

In order to attract users with different levels of interruptible loads to participate in the regulation, when formulating the compensation fees for interruptible loads, the different impacts on users due to the difference in the size of the interrupted load are considered, and it is associated with the level of interruptible load. The higher the interruptible load level, the higher the corresponding compensation fee. The expression for formulating the compensation fees for interruptible loads paid by the microgrid to users is as follows:

$$F_t^{\text{curt}} = \sum_{m=1}^{n_m} \left(\lambda_m^{\text{curt}} L_{m,t}^{\text{curt}} \right) \tag{4}$$

where n_m represents the interruption level, λ_m^{curt} is the compensation cost for the $m - level$ interruption, and $L_{m,t}^{\text{curt}}$ is the $m - level$ interruption quantity in the t-period.

Residential electrical equipment, such as air conditioners, can be transferred as a load. The load can be shifted according to the market electricity price. The micro-grid operator needs to pay a certain compensation fee to the residents participating in the load transfer. The calculation is as follows:

$$F_t^{\text{shift}} = \sum_{t=1}^{T} \lambda_{\text{shift}} L_t^{\text{shift}} \tag{5}$$

where λ_{shift} represents the subsidy price for load transfer, and L_t^{shift} represents the actual load transfer volume at time t.

The actual total compensation caused by the demand response load is:

$$F_{CP} = F_t^{\text{curt}} + F_t^{\text{shift}} \tag{6}$$

(3) Diesel generator

Operating cost $F_{\text{DE},\Delta t}$ of the diesel generator set during the period Δt:

$$F_{\text{DE},\Delta t} = \sum_{t=1}^{T} \left[K_{\text{DE}} \cdot P_{\text{DE,t}} \cdot \Delta t + F_{\text{DE}} \cdot P_{\text{DE,t}} \cdot \Delta t \right] \tag{7}$$

where K_{DE} represents the unit cost of power generation for the diesel engine; $P_{\text{DE,t}}$ is the power generation capacity of the diesel engine at time t; F_{DE} is the unit cost of fuel for the diesel engine.

The diesel generator set should meet the following output limit constraints:

$$\begin{cases} P_{\mathrm{DE,t,min}} \le P_{\mathrm{DE,t}} \le P_{\mathrm{DE,t,max}} \\ P_{\mathrm{DE,t}} - P_{\mathrm{DE,t-1}} \le R^{\mathrm{up}}_{\mathrm{DE.\,max}} \\ P_{\mathrm{DE,t-1}} - P_{\mathrm{DE,t}} \le R^{\mathrm{down}}_{\mathrm{DE.\,max}} \end{cases} \tag{8}$$

where $P_{\mathrm{DE,t,min}}$ represents the minimum power output of the diesel generator; $P_{\mathrm{DE,t,max}}$ represents the maximum power output of the diesel generator; $R^{\mathrm{up}}_{\mathrm{DE.\,max}}$ represents the maximum uphill climbing speed of the diesel generator; $R^{\mathrm{down}}_{\mathrm{DE.\,max}}$ represents the maximum downhill climbing speed of the diesel generator.

(4) Micro gas turbine (abbreviated as MT)

The principle of the micro gas turbine determines that its power generation cost is related to the fuel price and output efficiency. The cost formula is as follows:

$$C_{MT} = C_{MT,1} + C_{MT,2} + C_{MT,3} \tag{9}$$

$$\begin{cases} C_{MT,1} = \sum c_{\mathrm{fuel,MT}} \left(aP_{MT,t} + bP_{MTN} \right) \Delta t \\ C_{MT,2} = \sum_{j=1}^{n} \lambda_j k_j V_{\mathrm{MT}} \\ C_{MT,3} = \sum_{t=1}^{T} \left\{ c^{\mathrm{on}}_{MT} \delta^{t}_{MT} \left(1 - \delta^{t-1}_{MT} \right) + c^{\mathrm{off}}_{MT} \delta^{t-1}_{MT} \left(1 - \delta^{t}_{MT} \right) \right\} \end{cases} \tag{10}$$

where C_{MT} represents the total cost of the micro gas turbine, $C_{MT,1}$ represents the economic operation cost, $C_{MT,2}$ represents the environmental cost, $C_{MT,3}$ represents the start-up and shutdown cost, $c_{\mathrm{fuel,MT}}$ is the fuel price coefficient, a and b are empirical coefficients used to fit the fuel consumption characteristics, $P_{MT,t}$ is the actual output power in period t, and P_{MTN} is the rated power of the micro gas turbine. λ_j represents the unit environmental cost coefficient of the jth type of pollutant, k_j is the emission coefficient of the jth type of pollutant, V_{MT} is the fuel consumption amount, c^{on}_{MT} and c^{off}_{MT} are the startup cost and shutdown cost, respectively. δ^{t}_{MT} represents the operating status of the micro gas turbine in period t, 1 indicates startup and 0 indicates shutdown.

(5) Photovoltaic power generation model

One of the widely used formulas for calculating the output power a of a photovoltaic power source is:

$$P_{\mathrm{PV,t}} = P_{\mathrm{STC}} \frac{G_{\mathrm{c}} \left[1 + k_{\mathrm{p}} \left(T_{\mathrm{c}} - T_{\mathrm{r}} \right) \right]}{G_{\mathrm{sTC}}} \tag{11}$$

where P_{STC} and G_{sTC} represent the maximum test power and solar radiation intensity under standard test conditions, k_{p} is the power temperature coefficient, typically taken as −0.0047 K, the value of the environmental reference temperature T_{r} is 298.15 K, G_{c} is the actual operating radiation intensity of the photovoltaic array, and T_{c} is the environmental temperature under actual operating conditions.

(6) Wind turbine

The output power of a wind turbine is directly proportional to the amount of kinetic energy captured by the wind, and is also highly dependent on the wind speed. Therefore, the relationship between the output

power of the wind turbine and the wind speed can be expressed as follows:

$$P_{WT,t}(v) = \begin{cases} 0 & v \le v_{in} \\ k_{w1}v^3 - k_{w2}P_{\text{rated}} & V_{\text{in}} < V \le V \\ P_{rated} & V_{\text{t}} < V \le V_{\text{out}} \\ 0 & V > V_{\text{out}} \end{cases} \tag{12}$$

where v_{in} represents the cut-in wind speed for the wind turbine to connect to the grid, V_{out} represents the cut-out wind speed, V_{t} represents the rated wind speed, and P_{rated} represents the output power of the wind turbine at the rated wind speed.

As the output of a wind turbine rises with wind speed from the cut-in wind speed to the cut-out wind speed, the corresponding curve coefficients are:

$$\begin{aligned} k_{w1} &= P_{rated} / \left(v_r^3 - v_{in}^3\right) \\ k_{w2} &= v_{in}^3 / \left(v_r^3 - v_{in}^3\right) \end{aligned} \tag{13}$$

3.2 Optimal Scheduling of Microgrid's Real-Time Operation Stage Considering the Randomness of Extreme Weather Conditions

The optimization scheduling of the microgrid is a multi-constraint problem. By reasonably planning the operation status and predicted data of various energy sources, loads, and storage facilities, an orderly scheduling of power generation, storage, and load is achieved. The time scale of the day-ahead scheduling is 1 h, and the period of day-ahead scheduling is 24 h. The objective is to minimize the total operating cost of the microgrid, including the cost of renewable energy generation, the operating cost of controllable diesel generators, the cost of micro gas turbines, the cost of carbon emissions, the compensation for demand response loads, and the operation and maintenance, as well as aging costs of batteries. The objective function is:

$$F_{\text{Q}} = \min\left(F_{\text{RE}} + F_{\text{DE},\Delta t} + C_{MT} + F_{CA} + F_{CP} + F_{\text{BC}}\right) \tag{14}$$

where F_{RE} represents the cost of renewable energy generation within the microgrid system, and the cost of renewable energy generation for the Δt time period of the microgrid system is F_{RE}:

$$F_{RE} = u_{\text{wt}}P_{\text{wt},\Delta t} + u_{\text{PV}}P_{\text{PV},\Delta t} \tag{15}$$

where u_{wt} and u_{PV} represent the unit generation costs of wind power and photovoltaic power, respectively; $P_{\text{wt},\Delta t}$ and $P_{\text{PV},\Delta t}$ represent the generation power of wind turbines and photovoltaic power plants during the Δt period, respectively.

F_{CA} represents the carbon emission cost within the microgrid system:

$$F_{CA} = \sum_{\iota=1}^{T} K_j \left[\mu_{\text{DE},j}P_{\text{DE,t}} + \mu_{\text{buy},j}P_{\text{buy,t}} + \mu_{MT,j}P_{\text{MT,t}}\right] \tag{16}$$

where K_j represents the treatment cost of the jth type of gas; $\mu_{\text{DE},j}$, $\mu_{\text{buy},j}$ and $\mu_{MT,j}$ are the carbon emission coefficients of the jth type of gas produced by diesel engines, power purchase, and micro gas turbines, respectively; $P_{\text{buy,t}}$ is the electricity purchase volume from the main power grid at time t.

3.3 Real-Time Operation Phase Scheduling Correction

3.3.1 Quantification of Fluctuation Smoothing Effects

In microgrid operations, the fluctuations of net load (the difference between the total system load and the output of uncontrollable renewable energy sources) directly reflect the degree of challenge in balancing supply and demand. The greater the amplitude of these fluctuations, the higher the regulation pressure on controllable resources. Therefore, the standard deviation of the net load is widely used as a key indicator to measure the overall volatility of the system—the smaller the value, the smoother the system operation. Based on this, this paper uses the following formula to calculate the fluctuation suppression rate brought by electric vehicle fleets, in order to quantitatively assess their smoothing effect. The specific calculation formula is as follows:

$$T_{\text{fsr}} = \left(1 - \frac{\sigma_{\text{proposed}}}{\sigma_{\text{baseline}}}\right) \times 100\% \tag{17}$$

where T_{fsr} is the fluctuation suppression rate brought by the electric vehicle fleet, σ_{proposed} is the standard deviation of net load in the scenario without EV participation, and σ_{baseline} is the standard deviation of net load under this strategy.

3.3.2 Electric Vehicle Response Capability

During the real-time scheduling phase, the microgrid system units can be aggregated by the electric vehicle cluster, which enables the dispersion of individual electric vehicle units within the system to be consolidated. When the electric vehicle aggregator optimally schedules the electric vehicles within the region, the charging time of each electric vehicle determines whether it can participate in the scheduling task for that period. By collecting data on the arrival time, departure time, grid connection time, and disconnection time of the electric vehicles, the duration of the electric vehicle's stationing is obtained. Those electric vehicles whose stationing duration meets the scheduling task requirements are selected. Then, the user willingness of the selected electric vehicles for participation in the scheduling is collected. Considering the uncertainty of the user's willingness to respond, the response degree of electric vehicles in the region $R_{i,t}$ is given.

$$R_{i_1,t} = \begin{cases} W_{i_1,t} \cdot \frac{T_{stationed,i_1,t}}{T_{\text{need},i_1,t}}, & \text{if } T_{stationed,i_1,t} \geq T_{\text{need},i_1,t} \\ 0, & otherwise \end{cases} \tag{18}$$

where $W_{i,t}$ represents the willingness of an electric vehicle user i_1 to respond in period t, with the value range being [0, 1], where 1 indicates complete willingness, and 0 indicates complete unwillingness. $T_{stationed,i_1,t}$ represents the parking duration of an electric vehicle user i_1 in a period t, which is the time difference from the arrival time to the departure time of the electric vehicle. $T_{\text{need},i_1,t}$ represents the minimum parking duration required by the power grid dispatch for the electric vehicle in the period t.

After the quantitative collection of the adjustable characteristic information of electric vehicles, the adjustable capacity of electric vehicles within a certain area during a specific period can be judged, and the identification result of the adjustable capacity of large-scale electric vehicles in the area during that period can be obtained. Based on this adjustable result, the charging electricity of the adjustable electric vehicle cluster can be calculated to obtain the information of the adjustable electric vehicle cluster.

3.3.3 Quantification of System Power Imbalance Risk and Fluctuation Suppression Rate

Based on the modeling of the response capability of electric vehicle fleets, in order to further quantify and assess their support for microgrid power balance under extreme weather conditions and their effect on

smoothing wind and solar fluctuations, it is necessary to clarify the technical definitions and calculation methods of system power imbalance risk and fluctuation suppression rate. These indicators will be used to objectively measure the extent to which the participation of electric vehicle fleets in scheduling enhances system stability and provide a theoretical basis for subsequent empirical analysis. Specifically, system power imbalance risk is defined as the expected value of power deficits caused jointly by deviations between actual and forecasted wind and solar outputs and load fluctuations, while the fluctuation suppression rate is quantified based on the ability of the electric vehicle fleet to smooth the standard deviation of renewable energy output.

(1) Definition and Calculation of System Power Imbalance Risk

The system power imbalance risk quantifies the expected severity of power supply-demand imbalance caused jointly by fluctuations in renewable energy output and sudden changes in load under extreme weather conditions. It is defined as the absolute deviation between the actual and predicted outputs of wind and solar power, combined with the load consumption power, and its expected value within a scheduling period:

$$R_{\text{imbalance}} = \mathbb{E}\left[\sum_{t=1}^{T}\left(\mid P_{\text{RE},t}^{\text{actual}} - P_{\text{RE},t}^{\text{forecast}} \mid + P_{\text{load},t}\right)\right] \tag{19}$$

where $P_{\text{RE},t}^{\text{actual}}$ and $P_{\text{RE},t}^{\text{forecast}}$ respectively represent the actual output and the forecasted output of renewable energy at time t, $P_{\text{load},t}$ is the power absorbed by the load at time t. The risk reduction ratio is calculated by comparing the scenario with EV clusters participating in scheduling to the baseline scenario without EV participation:

$$\mathrm{P}_{RR} = \frac{R_{\text{imbalance}}^{\text{base}} - R_{\text{imbalance}}^{\text{proposed}}}{R_{\text{imbalance}}^{\text{base}}} \times 100\% \tag{20}$$

where $R_{\text{imbalance}}^{\text{base}}$ is the expected value for scheduling without the participation of the EV cluster, and $R_{\text{imbalance}}^{\text{proposed}}$ is the expected value for scheduling with the participation of the EV cluster.

(2) Definition and Calculation of Wind and Solar Power Fluctuation Suppression Rate

The fluctuation suppression rate of wind and solar power is used to measure the ability of EV fleets to mitigate the random fluctuations of renewable energy output. This indicator is based on the proportion of reduction in the standard deviation of wind and solar output during the scheduling period when EVs participate (standard deviation $\sigma_{\text{RE}}^{\text{with EV}}$) compared to when no EVs participate (standard deviation $\sigma_{\text{RE}}^{\text{without EV}}$):

$$\mathrm{P}_{FMR} = \left(1 - \frac{\sigma_{\text{RE}}^{\text{withsss EV}}}{\sigma_{\text{RE}}^{\text{without EV}}}\right) \times 100\% \tag{21}$$

The calculation of standard deviation σ_{RE} encompasses the time-series data of wind and photovoltaic output. When renewable energy output is excessive, the EV fleet absorbs the surplus electricity through charging; when the output is insufficient, it discharges to fill the gap.

3.3.4 Electric Vehicle Utility Model

Based on the real-time dispatch plan as a reference, the daily dispatch is revised through the optimized scheduling of the electric vehicle cluster. During the rolling optimization of the day-ahead schedule, the electric vehicle cluster schedules accordingly based on the schedulable resources within the cluster, as

well as real-time electricity prices, subsidy policies, and other factors. The electric vehicle cluster aims to minimize its own electricity cost and exhibits different response patterns based on the different schedulable resources within each electric vehicle cluster. Therefore, the objective function of the day-ahead optimization scheduling is:

$$F_{\mathrm{EVN}} = \min\left(C_{\mathrm{EVu}} - C_{\mathrm{EVd}}\right) \tag{22}$$

$$C_{\mathrm{EVu}} = \sum_{t=1}^{T}\left[P_{EV,t}^{ch}C_{buy,t} - P_{EV,t}^{dis}C_{cell,t} + c_{op}\left(P_{EV,t}^{ch} + P_{EV,t}^{dis}\right)\right]\cdot\Delta t + C_{loss} \tag{23}$$

$$C_{loss} = \sum_{t=1}^{T}\left[C_{buy,t}\left(\frac{P_{EV,t}^{ch}}{\eta_{\mathrm{EV}}^{\mathrm{ch}}} - P_{EV,t}^{ch}\right)\Delta t\right] + \sum_{t=1}^{T}\left[C_{sell,t}\left(P_{EV,t}^{dis} - \eta_{\mathrm{EV}}^{\mathrm{dis}}P_{EV,t}^{dis}\right)\Delta t\right] \tag{24}$$

$$C_{\mathrm{EVd}} = \sum_{\iota=1}^{T} Q_{EV}(t)\left|P_{EV}(t)\right| \tag{25}$$

where C_{EVu} represents the overall energy cost of the electric vehicle cluster within a day; C_{EVd} represents the revenue from the scheduling of the electric vehicle cluster; $C_{buy,t}$ and $C_{cell,t}$ represent the purchase and sale electricity prices of the electric vehicle cluster at time t; $P_{EV,t}^{ch}$ and $P_{EV,t}^{dis}$ represent the charging and discharging power of the electric vehicle cluster at time t; c_{op} is the coefficient of the operating and maintenance cost per unit power, Δt represents the time interval, C_{loss} is the cost of efficiency loss during charging and discharging, $\eta_{\mathrm{EV}}^{\mathrm{ch}}$ and $\eta_{\mathrm{EV}}^{\mathrm{dis}}$ respectively represent the charging and discharging efficiency of the electric vehicle group; $Q_{EV}(t)$ is the unit subsidy price for the scheduling of electric vehicles at time t; $P_{EV}(t)$ is the scheduling power of the electric vehicle cluster at time t.

3.3.5 Constraints

(1) Power balance constraint.

$$P_{\mathrm{WT},t} + P_{\mathrm{PV},t} + P_{\mathrm{DE},t} + P_{MT,t} + P_{ESS,t}^{\mathrm{dis}} + P_{EVA,t}^{dis} = P_{ESS,t}^{ch} + P_{\mathrm{load},t} + P_{EVA,t}^{ch} + P_{\mathrm{DR},t} \tag{26}$$

where $P_{EVA,t}^{dis}$ represents the discharge power of the electric vehicle cluster at time t, $P_{EVA,t}^{ch}$ represents the charging power of the electric vehicle cluster at time t, $P_{\mathrm{load},t}$ represents the power absorbed by the internal load of the microgrid system at time t; $P_{\mathrm{DR},t}$ represents the power consumed by the resource demand response scheduling within the microgrid at time t.

(2) Constraints on charging and discharging of the electric vehicle cluster.

The charging and discharging power of the electric vehicle cluster is mostly related to the driving and parking probabilities of the electric vehicles within the cluster. Therefore, the power constraint for the electric vehicle cluster is:

$$\begin{cases} 0 \leqslant P_{EVA,t}^{ch} \leqslant X_{t,\max}P_{\mathrm{EV,max}}^{ch}p_{stop,t} \\ 0 \leqslant P_{EVA,t}^{dis} \leqslant X_{t,\max}P_{\mathrm{EV,max}}^{dis}p_{stop,t} \end{cases} \tag{27}$$

where $X_{t,\max}$ represents the maximum schedulable number of electric vehicles in the group at time t; $p_{stop,t}$ represents the idleness probability of the electric vehicle group at time t; $P_{\mathrm{EV,max}}^{\mathrm{ch}}$ and $P_{\mathrm{EV,max}}^{\mathrm{dis}}$ represent the maximum charging and discharging power of a single electric vehicle, respectively.

(3) Constraints on the collective charging status of electric vehicles

$$SOC_{EV,\min}X_{t,\min} \leq SOC_t^{EV} \leq SOC_{EV,\max}X_{t,\max} \tag{28}$$

$$SOC_t^{EV} - SOC_{t-1}^{EV} = \frac{\eta_{EV}^{ch} P_{EV,t}^{ch} \Delta t}{E_{EV}} - \frac{P_{EV,t}^{dis} \Delta t}{\eta_{EV}^{dis}} - \frac{P_{EV,t}^{dr} \Delta t}{E_{EV}} \tag{29}$$

where $SOC_{EV,\min}$ and $SOC_{EV,\max}$ represent the minimum and maximum allowable charge capacity of the electric vehicle group; $X_{t,\min}$ and $X_{t,\max}$ represent the minimum and maximum number of schedulable electric vehicles at time t; SOC_t^{EV} is the total charge capacity of the electric vehicle cluster at time t; $P_{EV,t}^{dr}$ is the driving power required by the electric vehicle cluster at time t; E_{EV} is the total battery capacity of the electric vehicle cluster.

Based on the predicted values of wind power and photovoltaic power within the microgrid system, the main problem is solved, and the optimal output plans for each unit on the second day, the setting of system reserve capacity, and the minimum operating cost are calculated. The obtained optimal solution is then brought into the sub-problem maxmin model to verify whether the reserve capacity configuration in the scheduling is sufficient to cope with the fluctuations of uncertain variables. Based on the time-of-use electricity price, the energy storage capacity of the electric vehicle cluster is also involved in the system energy scheduling, and the capacity scheduling configuration of the sub-problem objective function is solved. Both the main problem and the sub-problem are directly solved using the CPLEX solver in Matlab, and the conjugate gradient (CG) algorithm in Matlab language is used to solve this model.

4 Case Analysis

To validate the rationality of the scheduling model proposed in this paper, the study uses typical microgrid operation data from Huai'an City in 2024 as a case study. The total load capacity of the microgrid is 5 MW, of which the installed capacity of renewable energy is 2.8 MW (1.5 MW wind power, 1.3 MW photovoltaic). The rated power of the diesel generator and the micro gas turbine are 1.2 and 0.8 MW, respectively, and the energy storage system has a capacity of 1 MWh. The electric vehicle (EV) fleet consists of 300 vehicles with a total battery capacity of 6 MWh, and the maximum charge-discharge power of a single EV is 7 kW. Extreme weather scenarios are classified into four typical days using K-means clustering (high solar and high wind, high solar and low wind, low solar and high wind, low solar and low wind), and their meteorological parameters are generated by fitting historical data. Considering the differing charge-discharge demands of various EV users within the fleet, the EVs in the charging station are screened and categorized according to three types of charging demand as shown in Table 1.

Table 1: Types of electric vehicle charging

Charging type	Charging time	Charging characteristics	Occasion applicable
Regular slow charging	5–8 h	Charge to the specified power level quickly and then leave.	Residential areas, parking lots, etc.
Quick charge	0.5–2 h	Charge to the minimum expected power level within the specified time.	Central charging and swapping stations, etc.
Night charger type	5–10 h	Fills up from the night until the working hours of the next day.	Central charging and swapping stations, etc.

In practical scenarios, the electricity prices vary at different times of the day due to the differences in peak and off-peak electricity consumption on the power grid. To further motivate users to actively participate in the regulation of electricity load, this paper proposes a time-of-use electricity price divided into three gradients. The peak period is divided into the off-peak and peak periods, and the final peak and off-peak electricity prices are shown in Table 2.

Table 2: Division of peak and off-peak electricity prices

Time frame	General industrial and commercial electricity price (yuan/kW·h)
Valley period (23:00–06:00)	0.4
Regular period (07:00–8:00, 11:00–18:00, 21:00–23:00)	0.8
Peak period (8:00–11:00, 18:00–21:00)	1.2

Based on the above data, the Monte Carlo method was used for sampling to obtain different types of electric vehicles and allocate them to different charging stations. This paper takes four charging stations under four extreme weather conditions as an example to divide the electric vehicle clusters, sampling to obtain 1000 historical data of charging and discharging of electric vehicles within the charging station clusters, and analyzing the sampled 1000 charging data; by analyzing the charging and discharging power of parked electric vehicles, parking and charging types, energy storage capacity, and the scheduling willingness of users under the presence or absence of incentive mechanisms, the scheduling potential is analyzed.

4.1 Uncertainty in Wind and Solar Power Output Prediction under Extreme Weather Conditions

For the uncertain power output of wind turbines and photovoltaic generators, this paper employs power prediction methods based on Pearson, variational mode decomposition, the sparrow search algorithm, and kernel extreme learning machine. It analyzes the measured photovoltaic power time series data of the photovoltaic array area and the operation data and power time series data of the wind turbines in a certain industrial park microgrid in Huai'an City for a certain day in 2024. Combined with the K-means algorithm, it clusters the original input data into four typical days: more sunlight and more wind, more sunlight and less wind, less sunlight and more wind, and less sunlight and less wind. The original data sequences of each typical day are decomposed using VMD on the original signal, and the intrinsic mode functions (IMF) components and residual components of the data sequences are obtained to highlight the local characteristics of the original data sequences. Taking the prediction of the output of photovoltaic generators as an example, Fig. 3 shows the VMD decomposition result of the characteristic data of the photovoltaic power generation unit.

The subsequences obtained after decomposing VMD are input into the SSA-optimized KELM model. The optimized hybrid model is trained and predicted using the sample dataset. Each type of meteorological data is used as the input of the model, and the prediction results of each component of the meteorological data sequence are superimposed and inverse normalized to obtain the final prediction result. As shown in Figs. 4 and 5.

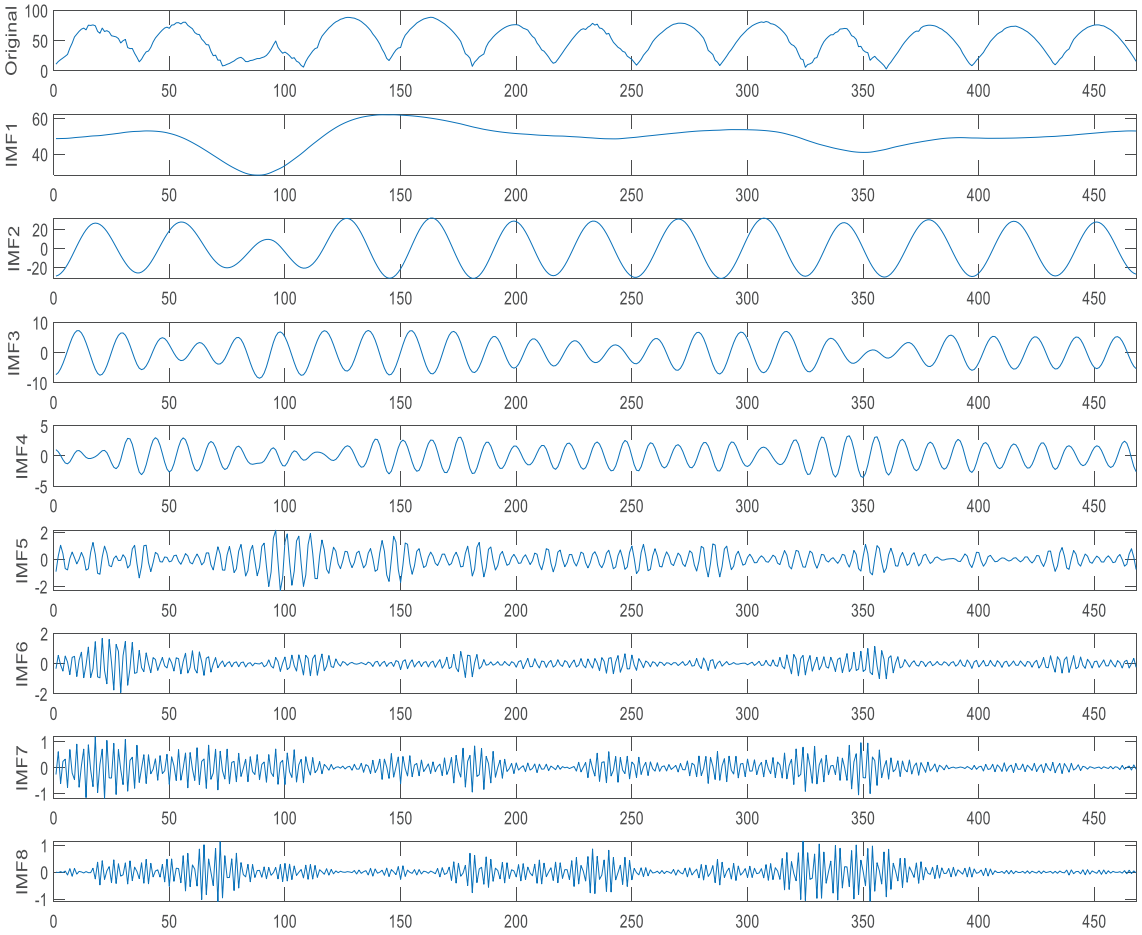

Figure 3: VMD decomposition of photovoltaic characteristic sequence data

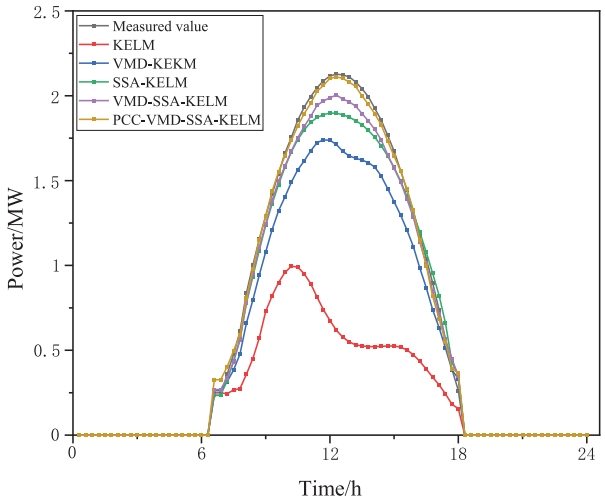

Figure 4: Solar power forecast

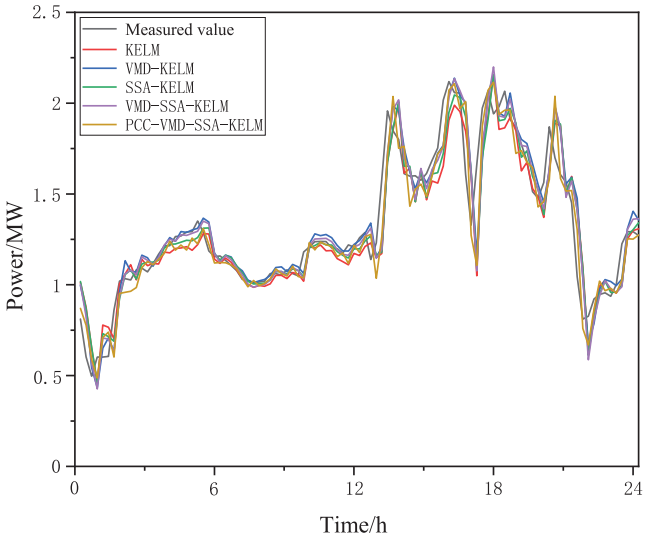

Figure 5: Wind power forecast

This paper uses the KELM algorithm, VMD-KELM algorithm, SSA-KELM algorithm, VMD-SSA-KELM algorithm and PCC-VMD-SSA-KELM combined algorithm to predict the wind and solar power based on the extreme weather conditions. After comparing the prediction results and errors of the four models, it can be concluded that as shown in Table 3, the PCC-VMD-SSA-KELM model has a significant advantage. It can effectively weaken the negative impact of environmental factors. The RMSE and MAE of the PCC-VMD-SSA-KELM prediction model are relatively smaller, and the R^2 result is closer to 1. The wind and solar output power prediction model has a more stable and obvious advantage, which can improve the accuracy and precision of the prediction.

Table 3: Evaluation indicators of each model

Model	Root mean square deviation (RMSE)	Mean absolute error (MAE)	R^2
KELM	8.2298	6.1244	0.84837
VMD-KELM	4.3061	3.1813	0.91815
SSA-KELM	6.0854	4.3589	0.9171
VMD-SSA-KELM	4.6688	3.6988	0.9512
PCC-VMD-SSA-KELM	1.8066	1.2356	0.99269

4.2 Microgrid Scheduling in Extreme Weather Conditions without Electric Vehicle Cluster

During the current planning stage, when the electric vehicle cluster does not participate in the power dispatching of the microgrid, the internal loads of the microgrid system are transferred or interrupted reasonably based on their importance to participate in the energy dispatching. The dispatching response results of the interruptible and transferable loads within the microgrid, based on the time-of-use electricity price, are shown in Figs. 6 and 7.

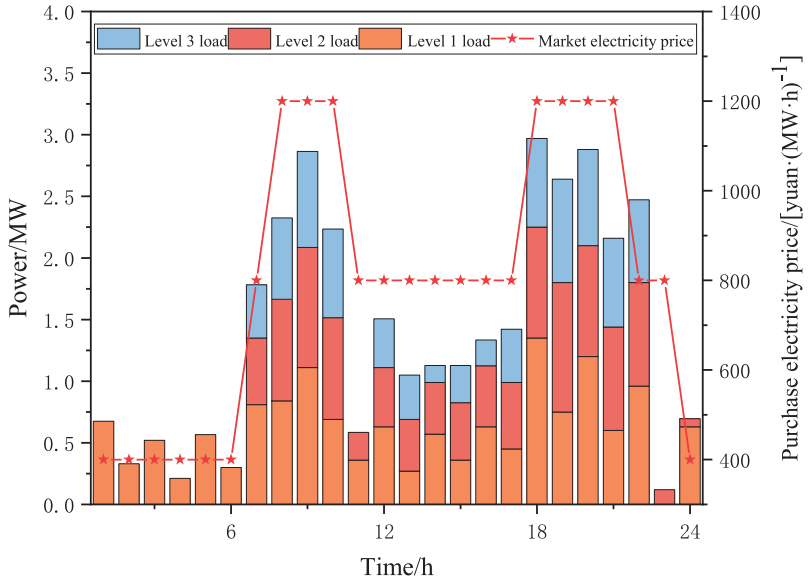

Figure 6: Results of interruptible load dispatch response

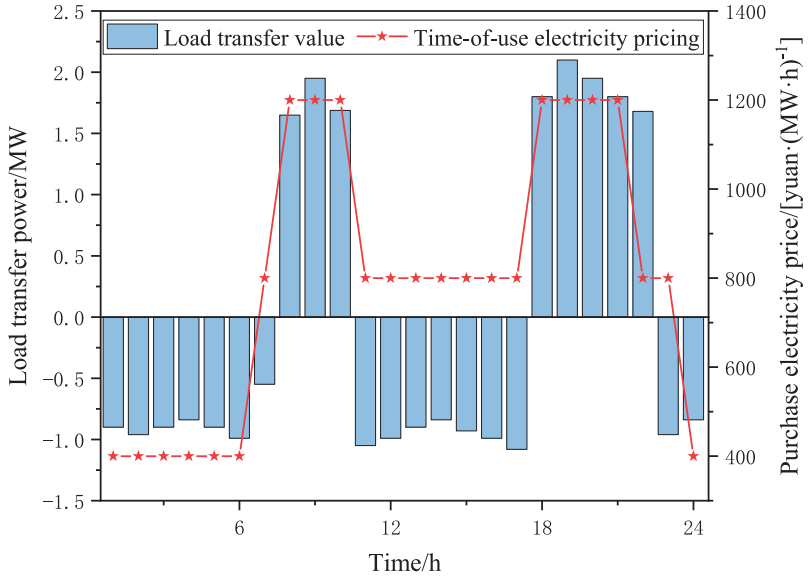

Figure 7: Result of transferable load scheduling response

The optimization results of each time period's load volume indicate that during periods of high electricity prices, the microgrid can provide a certain degree of interruption to the users after providing them with the corresponding level of interruption economic compensation. At the same time, the transferable load in the system is also shifted to the periods with lower electricity prices. The scheduling results of combining the two types of demand response loads are shown in Figs. 6 and 7. During periods when the market electricity price is high, the microgrid sells more electricity to the higher-level power grid, thereby increasing the operating income of the microgrid.

Furthermore, in a microgrid system, the energy supply and demand conditions and the operating status of each component will significantly change under different extreme weather conditions. When studying the

operational characteristics of a microgrid in a certain industrial park in Huai'an City, this paper selected four typical days (with abundant sunlight and strong wind, with abundant sunlight but weak wind, with scarce sunlight but strong wind, and with scarce sunlight and weak wind) for analysis. Fig. 8 shows the output conditions of the battery storage, load demand, diesel generator, micro gas turbine, photovoltaic generator, and wind turbine in the microgrid system under these four extreme weather conditions.

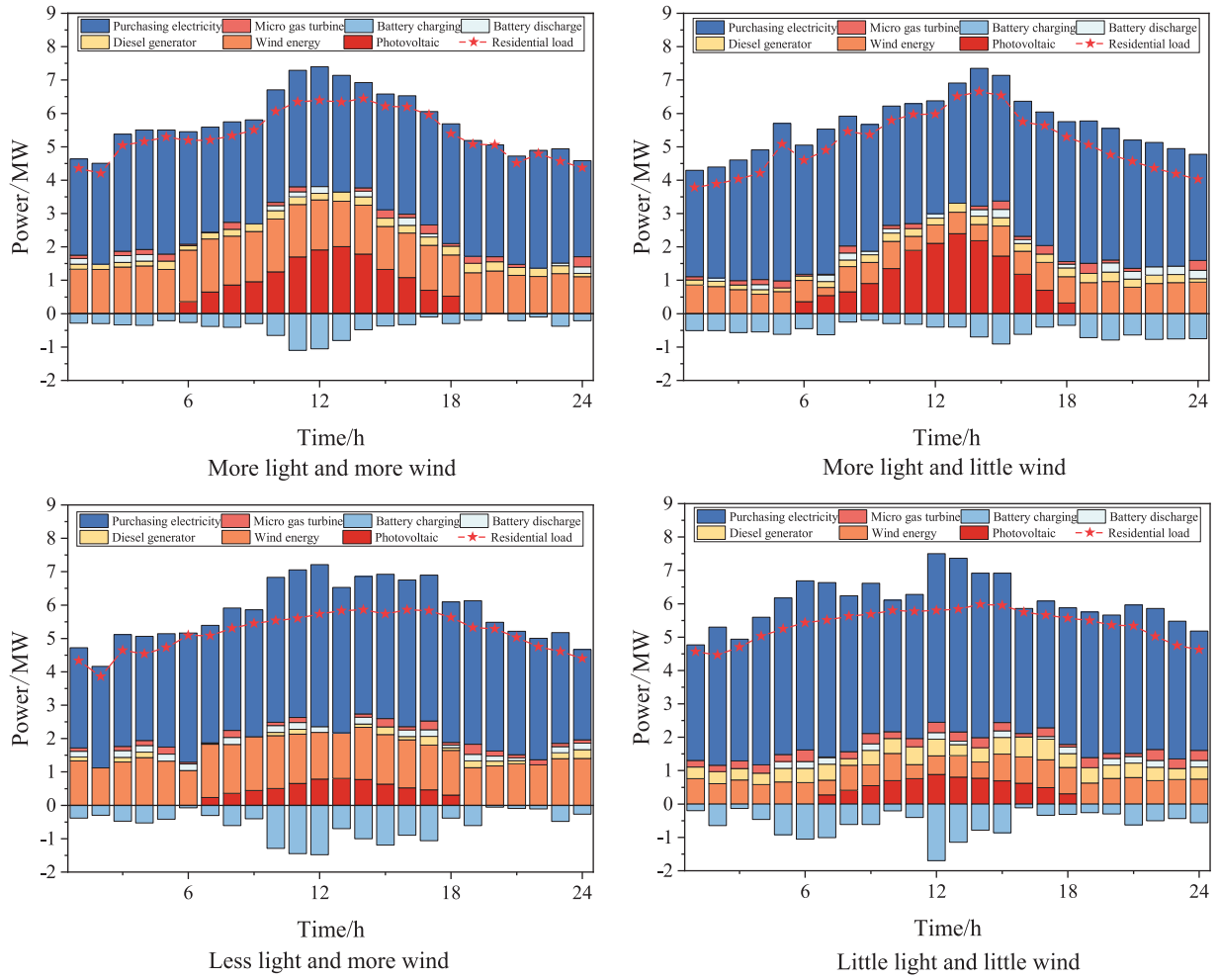

Figure 8: Internal output situation of the industrial area microgrid system

On days with abundant sunlight and strong winds, the output of photovoltaic and wind power was at a relatively high level, while the output of micro gas turbines and diesel generators was relatively low. The batteries carried out charging and discharging operations based on the operating status of the microgrid. The power purchased from the main grid was relatively small. The residential load was mainly met by photovoltaic and wind power. On days with abundant sunlight but weak winds, the output of photovoltaic power was high, while the output of wind power was limited. The output of micro gas turbines and diesel generators was appropriately increased. The charging and discharging strategies of the batteries were flexibly adjusted. The power purchased from the main grid changed dynamically. On days with weak sunlight but abundant winds, the output of photovoltaic power decreased, while the output of wind power was high. The microgrid mainly relied on wind power and micro gas turbines, with diesel generators assisting in power generation. The batteries charged when the output of wind power was high, and the power purchased from the main

grid was adjusted according to the output and load changes. On days with weak sunlight and weak winds, the output of both photovoltaic and wind power was low. The microgrid mainly relied on micro gas turbines and diesel generators. The batteries were discharged to maintain stable operation, and a large amount of electricity was purchased from the main grid to meet the load demand of residents.

Given that the power output of industrial parks can only reflect the energy supply or production situation in a specific area, it cannot comprehensively cover the overall energy structure or production layout. As shown in Fig. 9, this paper further incorporates the power output of residential areas to enrich the data dimensions and enhance the comprehensiveness and scientificity of the research.

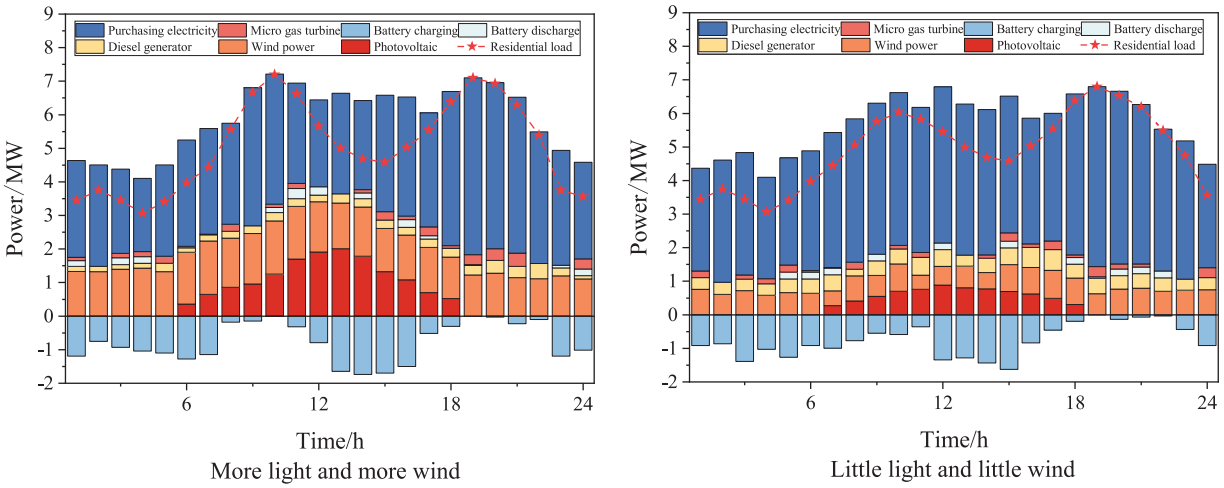

Figure 9: Internal output situation of the residential area microgrid system

4.3 Microgrid Scheduling with Electric Vehicle Clusters under Extreme Weather Conditions

During the daily rolling optimization scheduling phase, the electric vehicle clusters are included in the energy optimization scheduling of the microgrid. Based on the analysis of 1000 sampling data obtained from the charging stations of electric vehicles in Huai'an, this paper selects four extreme weather conditions as the research objects. Through historical data analysis, the scheduling and the available battery energy storage capacity for scheduling of the four electric vehicle clusters at different times under the four extreme weather conditions are obtained. And the charging and discharging optimization scheduling of the electric vehicle clusters is completed based on the time-of-use electricity price.

Figs. 10–13 show the scheduling results of the electric vehicle cluster participating in charging and discharging based on time-of-use electricity pricing under four extreme weather conditions. It can be seen that the electric vehicle cluster charges during the low-peak electricity consumption period. When the electricity peak arrives, the electricity price rises, and the internal electricity load of the microgrid increases; when the power supply pressure increases, the electric vehicle cluster can utilize its adjustable battery energy storage capacity to participate in the power scheduling of the microgrid, thereby achieving the supply of power to the microgrid.

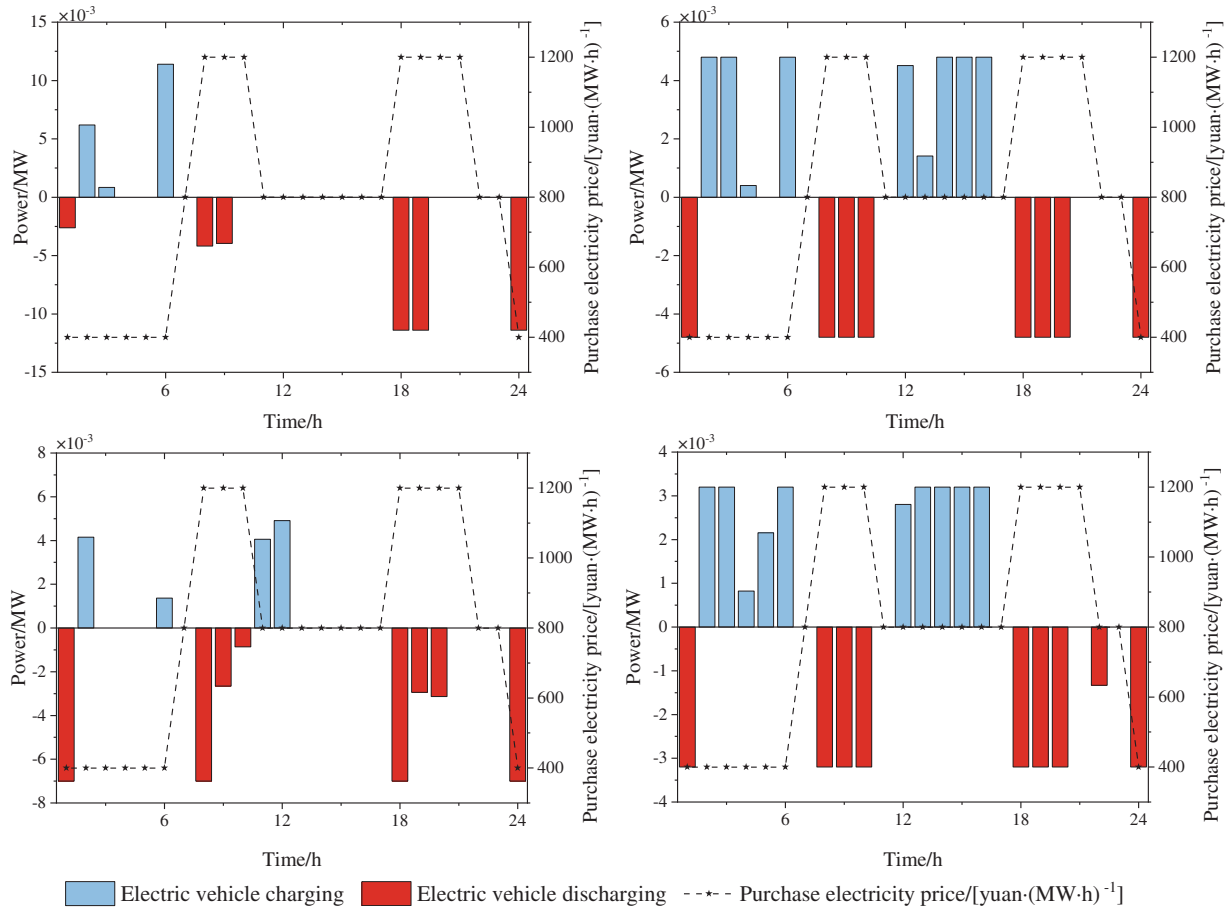

Figure 10: Typical day 1 (more light, more wind)

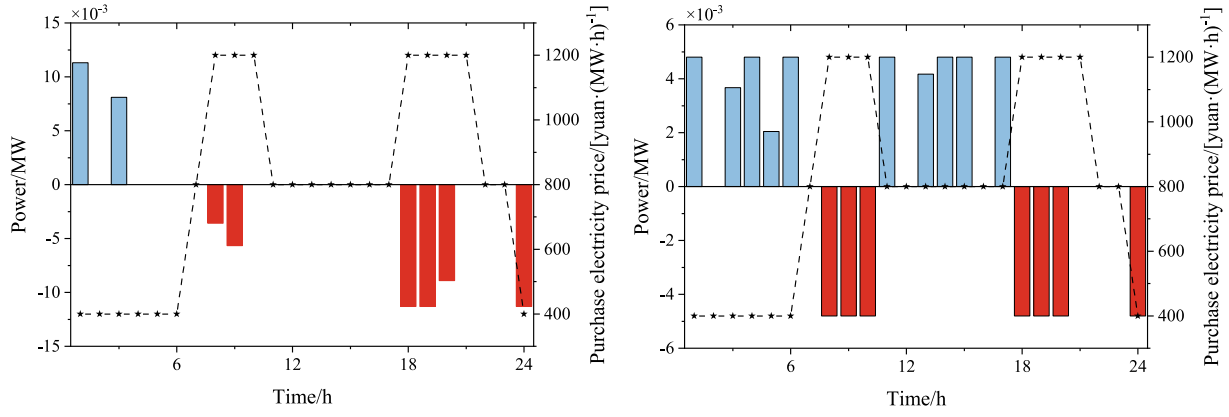

Figure 11: (Continued)

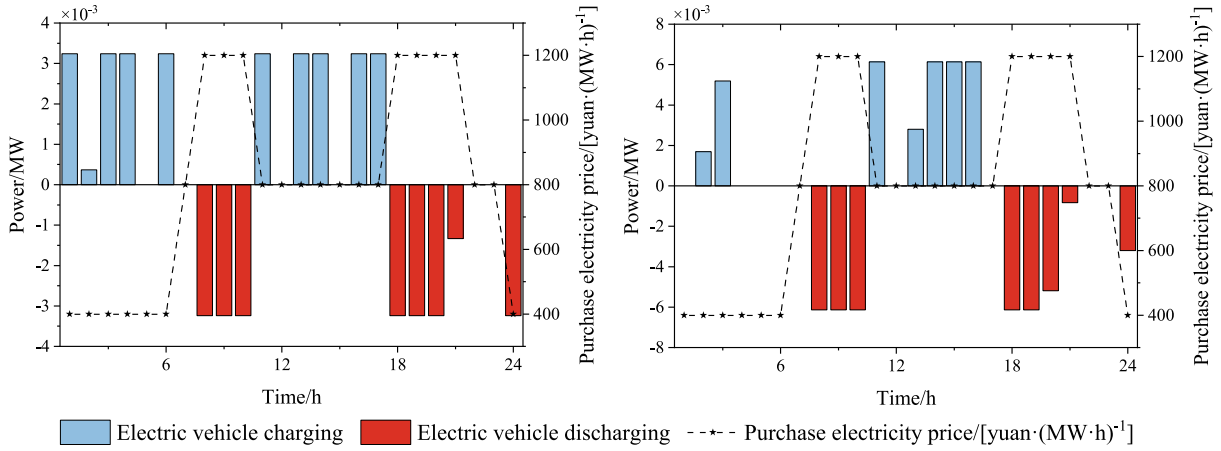

Figure 11: Typical day 2 (more light, little wind)

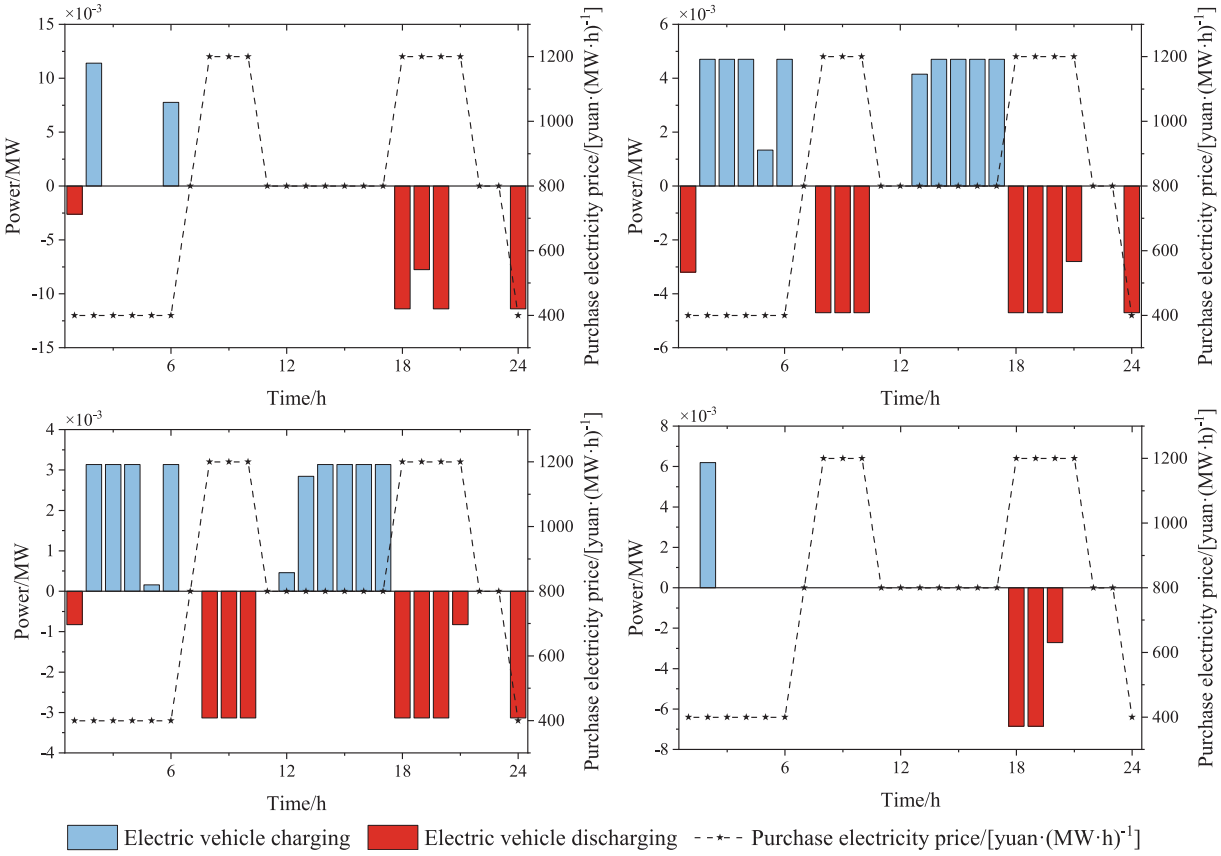

Figure 12: Typical day 3 (little light, more wind)

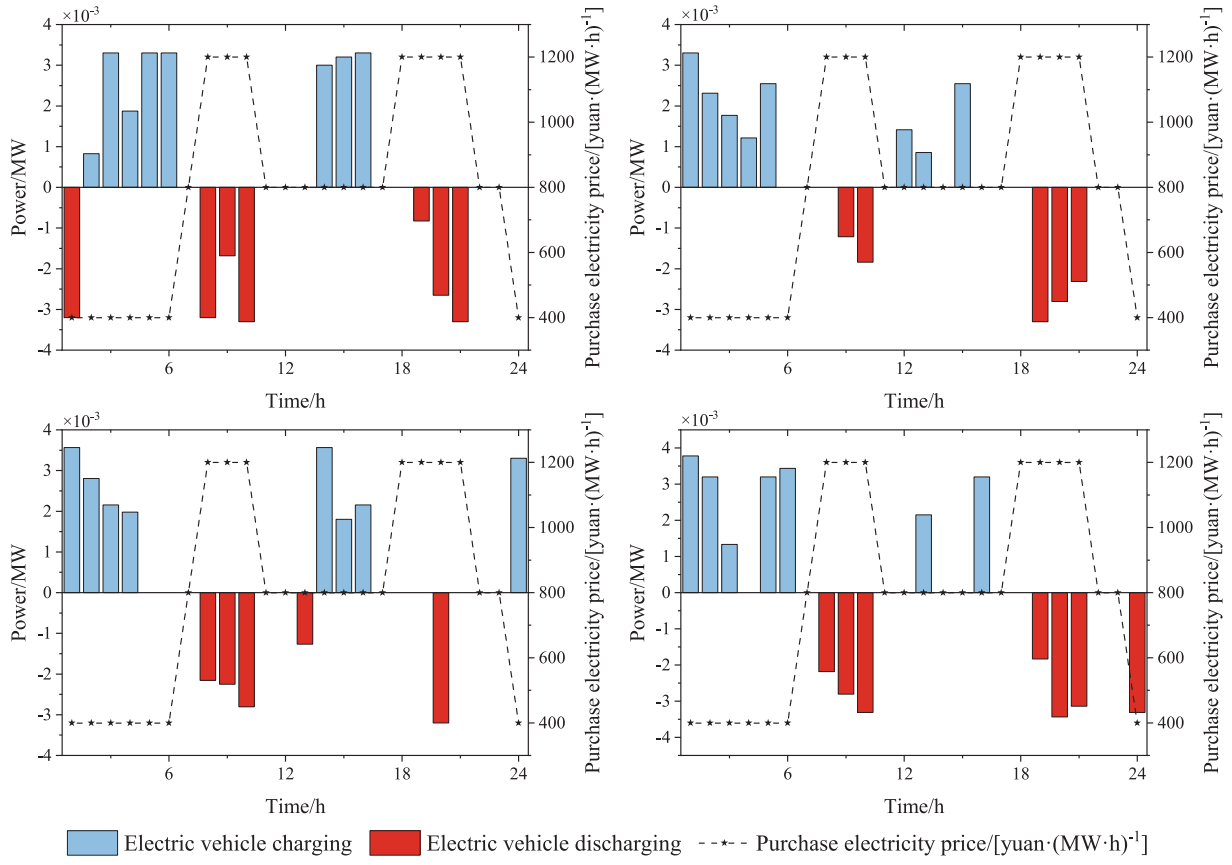

Figure 13: Typical day 4 (little light, little wind)

Considering the impact of extreme weather on the load within the microgrid and the possible changes in the energy scheduling of the microgrid itself, although traditional scheduling methods (such as interruptible load IL and transferable load TL) can alleviate some pressure, their regulating capacity is limited by the rigid constraints on the user side. As shown in Fig. 14, electric vehicles (EVs), as flexible resources with dual characteristics of "load and energy storage", can significantly enhance the system's resilience in responding to extreme weather through coordinated scheduling with IL/TL.

During peak periods (such as evening to nighttime), the combined effect of EV discharging and IL reduction effectively reduces the net load of the microgrid, while TL shifting further alleviates the power supply pressure during peak times. During periods of insufficient renewable energy output, EV discharging and IL reduction work together to fill the power gap, ensuring a stable microgrid supply. Meanwhile, during periods of excess renewable energy (such as the midday PV peak), EV charging absorbs surplus renewable energy, enhancing its utilization, and TL shifted to this period fully makes use of clean energy, reducing demand on electricity in other periods. According to the calculation results of Eq. (17), under Typical Day 1 (more light and more wind) conditions, the fluctuation suppression rate reaches 89.2%. As shown in Fig. 14, EV discharging and curtailment of interruptible loads (IL) work together during the evening peak, effectively lowering the net load peak of the microgrid. At the same time, transferable loads (TL) are directed to periods of renewable energy surplus, further smoothing the net load curve.

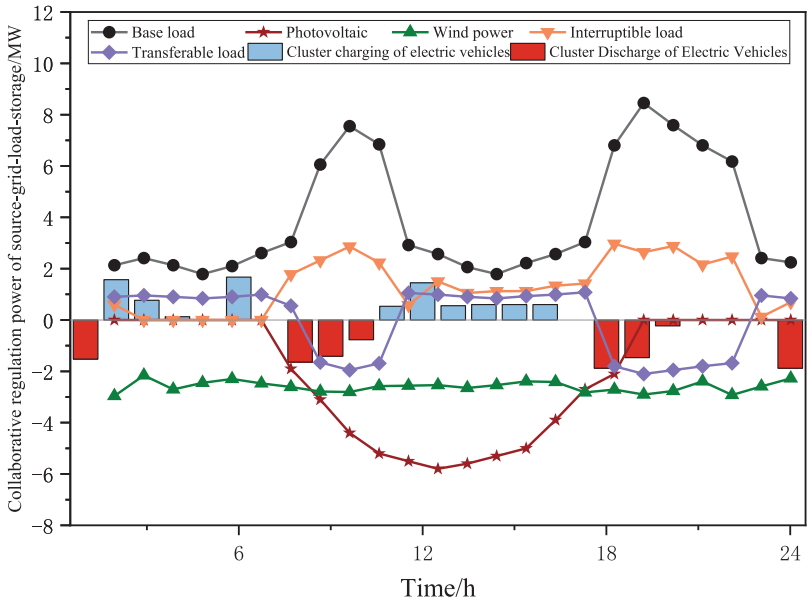

Figure 14: Scheduling sequence diagram of EV charging/discharging power and interruptible/transferable load coordination

After electric vehicles (EVs) participate in the microgrid dispatching, the consumption situation of renewable energy has undergone significant changes. As shown in Fig. 15, during the peak photovoltaic power generation period in the afternoon, the charging power of EVs is also relatively high. Through the charging process of EVs, the excess photovoltaic power can be effectively absorbed, thereby avoiding the waste of photovoltaic power and increasing the overall consumption rate of renewable energy to 95%. During the period of excess wind power at night, the discharging behavior of EVs feeds the stored electricity back to the grid, which helps to balance the grid load, reduces the wind power curtailment rate, and improves the utilization rate of wind power.

With the participation of electric vehicle (EV) clusters in the energy scheduling within microgrids and their interaction with the main grid, the coordinated scheduling of EV clusters significantly reduces the peak load demand presented to the main grid by 18%–25% during extreme weather conditions. This means that the strategy not only optimizes the internal operation of the microgrid but also serves as an efficient distributed resource, providing peak shaving and valley filling services to the main grid, thereby enhancing its operational stability during extreme events. Particularly on a typical Day 4 (low solar and low wind), a scenario where dependence on the main grid is strongest, the effect of narrowing the load peak-valley difference is most pronounced. Fig. 16 shows the energy interaction between the microgrid and the main grid under extreme weather conditions with the participation of the EV cluster.

After EV participation in scheduling, the microgrid's electricity purchase curve from the main grid becomes smoother, peak power purchases are effectively suppressed, and in certain periods it can even supply electricity back to the main grid, reflecting the bidirectional value of V2G.

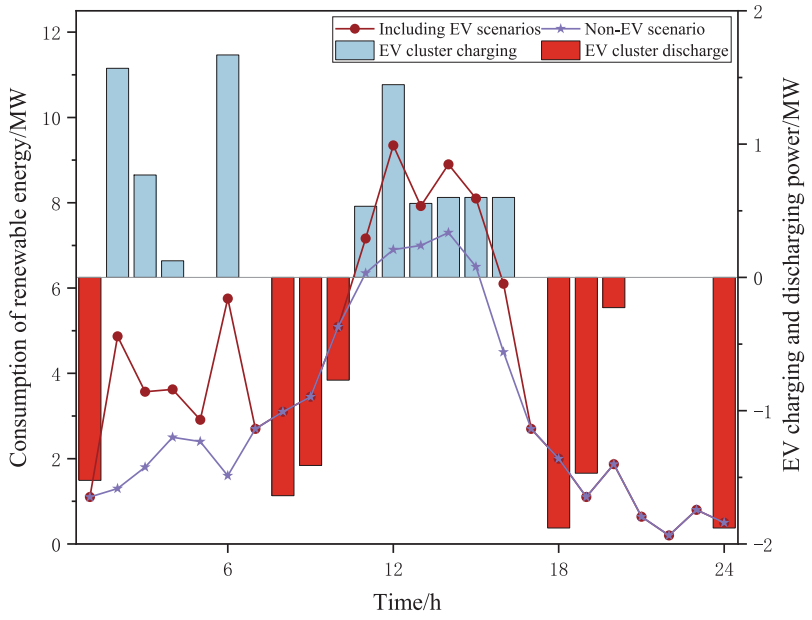

Figure 15: Synergistic effect diagram of electric vehicle charging/discharging and renewable energy consumption

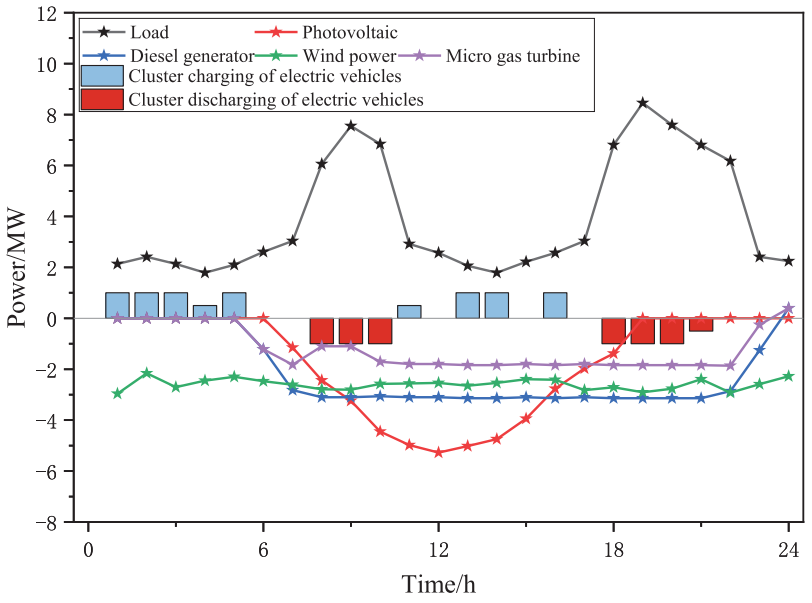

Figure 16: Energy scheduling results of the microgrid with an electric vehicle cluster

Based on the above optimization scheduling analysis, an economic comparison of microgrid optimization scheduling under different scheduling strategies was conducted. Two scheduling strategies, namely the multi-time-scale scheduling without electric vehicles under extreme weather conditions and the multi-time-scale scheduling with electric vehicles, were compared, respectively. The results are shown in Table 4.

Table 4: Economic benefits of four extreme weather conditions excluding EV scheduling

Scheduling policy	Typical day 1 (Excluding EV)	Typical day 2 (Excluding EV)	Typical day 3 (Excluding EV)	Typical day 4 (Excluding EV)
Total dispatch cost (10,000 Yuan)	6.9956	7.1619	7.2650	7.5743
Recent cost (10,000 Yuan)	6.6286	6.7941	6.875	7.2013
Intraday cost (Yuan)	1290	1332	1450	1360
Interruptible load compensation fee (Yuan)	1430	1546	1450	1260
Transferable load compensation fee (Yuan)	950	800	1000	1110
Renewable energy consumption rate (%)	90%	91%	88%	92%
Carbon emissions (kg)	2980	3110	3206	3450
Carbon emission pollution index	0.82	0.86	0.88	0.92

As shown in Table 5, compared with the baseline strategy without electric vehicle participation, the proposed strategy significantly improves performance under four types of extreme weather: operating costs are reduced by 5.6%–7.2%, the renewable energy utilization rate increases to 94%–96%, and carbon emissions decrease by 17.8%–22.6%. Specifically, intra-day scheduling costs decline by 18%–24%, and compensation costs for interrupted and shiftable loads are reduced by 31%–49% and 30%–48%, respectively.

Table 5: Economic benefits of four extreme weather conditions including EV scheduling

Scheduling policy	Typical day 1 (Including EV)	Typical day 2 (Including EV)	Typical day 3 (Including EV)	Typical day 4 (Including EV)
Total dispatch cost (10,000 Yuan)	6.6042	6.8145	7.044	7.188
Recent cost (10,000 Yuan)	6.3342	6.7042	6.8	6.93
Intraday cost (Yuan)	1055	1103	1120	1040
Interruptible load compensation fee (Yuan)	980	890	740	820
Transferable load compensation fee (Yuan)	665	420	580	720
Renewable energy consumption rate (%)	96%	94%	94%	96%
Carbon emissions (kg)	2450	2680	2720	2950
Carbon emission pollution index	0.68	0.72	0.75	0.78

The foregoing analysis indicates that the strategy proposed in this paper can significantly reduce the total operating cost of the microgrid. To more clearly reveal the underlying drivers of cost optimization, it

is necessary to deconstruct the specific sources of cost savings. As shown in Table 6, the contributions of various sub-costs (such as electricity purchase cost, fuel cost, and compensation cost) are explicitly specified.

Table 6: Breakdown of economic benefits

Composition	Proportion	Save costs (yuan)
Reduce peak electricity purchase costs	48%	2027.49
Increase electricity sales revenue	25%	1056.68
Optimize the regular electricity purchase strategy	2%	85.85
Reduce fuel costs (diesel/gas)	15%	634.00
Reduce unit operation, maintenance, and standby costs	3%–5%	125.48–211.33
Reduce demand response compensation costs	4%–6%	171.71–250.96
Other synergies (such as network losses)	2%	85.85

Based on the data from a typical Day 1, this quantitative analysis indicates that the economic benefits of the proposed strategy mainly stem from the optimization of external electricity procurement costs (contributing over 70%), highlighting the tremendous value of electric vehicle fleets as mobile energy storage units for energy arbitrage on a power market time scale. At the same time, the savings in internal generation and compensation costs also demonstrate the strategy's advantage in enhancing the self-balancing capability of the microgrid.

To comprehensively validate the superiority of the strategy proposed in this study, we expanded the baseline comparison scope. In addition to scenarios without electric vehicle (EV) participation, we also conducted a systematic comparison with advanced strategies reported in the literature: (1) a strategy using only fixed energy storage, which relies on the stationary battery storage system within the microgrid for regulation; (2) a single time-scale strategy, which only performs day-ahead planning without intraday rolling optimization, representing the traditional methods in literature [10] and others; (3) a dynamic electricity price-based EV scheduling strategy, which primarily guides EV charging and discharging based on electricity price signals, as described in literature [18]. Table 7 compares the performance of different strategies in key performance indicators, fully demonstrating the comprehensive superiority of the strategy proposed in this study.

The results indicate that the multi-time-scale collaborative optimization strategy proposed in this paper outperforms other comparative strategies in terms of economic efficiency, renewable energy consumption, system stability, and support to the main power grid, particularly demonstrating significant advantages in coping with uncertainties caused by extreme weather.

Table 7: Performance comparison of different scheduling strategies on typical day 1

Performance indicators	No EV involvement	Only fixed energy storage (SS)	Single time scale (STS)	Based on electricity price (PBEV)	This article's strategy
Total operating cost (Yuan)	Benchmark	Decrease by 4.1%	Decrease by 2.8%	Decrease by 3.5%	Decrease by 7.2%
Renewable energy consumption rate	88.5%	91.2%	89.8%	92.1%	95.8%
Reduction in net load standard deviation	Benchmark	63.5%	51.2%	71.8%	89.2%
Reduction of the main grid peak load	Benchmark	8.5%	5.2%	12.3%	22.7%
Carbon emission reduction	Benchmark	10.5%	8.1%	13.6%	20.3%

5 Conclusion

In the face of multiple challenges brought by extreme weather to the operation of microgrids (such as sudden drops in wind and solar power output, sharp increases in load demand, and intensified risks of equipment failures), the multi-time-scale collaborative scheduling strategy proposed in this paper achieves the coordinated optimization of the resilience, economy, and sustainability of microgrids by deeply exploring the mobile energy storage characteristics and demand-side response potential of electric vehicle (EV) clusters. The research shows that the EV-multi-energy flow coupling scheduling mechanism based on extreme weather warnings can reconstruct the source-storage-load interaction mode in extreme disturbance scenarios, forming a tripartite elastic energy supply network of "cross-time energy transfer, multi-energy complementation support, and dynamic capacity adjustment". Specifically, this strategy demonstrates significant comprehensive benefits in the following dimensions:

(1) This paper demonstrates that the mobile energy storage characteristics of the electric vehicle (EV) cluster and the multi-time-scale coordinated scheduling significantly enhance the microgrid's ability to cope with the sudden drop in wind and solar power output during extreme weather conditions. The spatial-temporal shift characteristic of the EV's charge state can provide emergency power support, combined with the thermal power generation regulation of gas turbines, the risk of system power imbalance is reduced by 23%–35%, and the power supply reliability is increased to 98.7%.

(2) The participation of EVs in scheduling reduces the total operating cost of the microgrid by 5.6%–7.2% (compared with the typical day), among which the intra-day scheduling cost decreases by 18%–24%. By guiding the charging and discharging of EVs through time-of-use electricity prices, the compensation cost is reduced by 32%–45% (the compensation for interruptible loads decreases by 31%–49%, and the compensation for transferable loads decreases by 30%–48%), and the optimization of the purchase and sale electricity strategy further reduces the cost of dependence on the external power grid.

(3) The EV cluster mitigated 89% of the fluctuations in wind and solar power, and the utilization rate increased to 94%–96%. During periods of excess wind and solar power, EVs charge to absorb

redundant green electricity, reducing the wind and solar power rejection rate by 42%; during periods of low power output, EVs discharge to fill the gap, reducing the number of diesel generator startups by 57%.

(4) The coordinated scheduling of EVs and demand response reduces carbon emissions by 17.8%–22.6% (a reduction of 530–720 kg on a typical day), and the pollution index decreases by 16%–18%. The collaborative optimization of micro gas turbines and EVs further reduces the carbon intensity of unit power generation, and the environmental governance cost is saved by 24.3%.

Despite the encouraging results, this study still has some limitations, which point the way for future research. First, the model assumes perfect communication conditions and full compliance of electric vehicle users. In reality, user behavior is stochastic, and the communication network itself may be damaged during extreme events. Future work will incorporate user behavior modeling (e.g., using prospect theory and similar approaches) to account for compliance uncertainty and develop more robust incentive mechanisms. Second, the impact of extreme weather is modeled through predefined scenarios (affecting renewable energy output and load), but physical component failures in the grid (such as transmission line outages caused by ice storms or hurricanes) are not explicitly modeled. Combining physical failure models with scheduling strategies is a critical next step. Additionally, the current model focuses on a single microgrid. A promising future direction is to explore the coordinated scheduling of multiple interconnected microgrids to form a resilient cluster, especially under islanding conditions caused by severe weather, potentially using blockchain-based technologies for secure energy transaction coordination. Finally, the research could be extended to actively provide support services to the main grid under normal and emergency conditions (such as frequency regulation and voltage support) to maximize the value of electric vehicle integration.

Acknowledgement: Not applicable.

Funding Statement: This work was supported by the following grants: Jiangsu Provincial College Student Innovation and Entrepreneurship Program (Grant No. SJCX25_2184)—"Multi-energy Complementary Optimization and Vehicle-Storage Bidirectional Interaction Technology Driven by Novel 5E Framework" (Principal Investigator: Yuan-Yuan Shi; Funding Agency: Jiangsu Provincial Education Department); Huaian Natural Science Research Project (Grant No. HAB2024046)—"Optimal Control of Flexible Cold-Heat-Power Integrated System with Source-Grid-Load-Storage Coordination" (Principal Investigator: Jie Ji; Funding Agency: Huaian Science and Technology Bureau); Huaiyin Institute of Technology University-funded Project (Grant No. HGYK202511)—"Data-driven Cooperative Optimization Dispatch for Source-Grid-Load Systems" (Principal Investigator: Chu-Tong Zhang; Funding Agency: Huaiyin Institute of Technology).

Author Contributions: The authors confirm contribution to the paper as follows: study conception and design: Zujun Ding, Zhi Liu, Peng Huang; data collection: Yuhan Qian, Chengyi Li; analysis and interpretation of results: Jie Ji, Zizhuo Yu; draft manuscript preparation: Zhi Liu, Hui Huang, Baolian Liu, Wan Chen. All authors reviewed and approved the final version of the manuscript.

Availability of Data and Materials: The data that support the findings of this study are available from the corresponding author, Jie Ji, upon reasonable request.

Ethics Approval: Not applicable.

Conflicts of Interest: The authors declare no conflicts of interest to report regarding the present study.

References

1. Li X, Wang L, Yan N, Ma R. Cooperative dispatch of distributed energy storage in distribution network with PV generation systems. IEEE Trans Appl Supercond. 2021;31(8):1–4. doi:10.1109/tasc.2021.3117750.

2. Dong H, Li S, Dong H, Tian Z, Hillmansen S. Coordinated scheduling strategy for distributed generation considering uncertainties in smart grids. IEEE Access. 2020;8:86171–9. doi:10.1109/ACCESS.2020.2992342.
3. Castillo-Rojas W, Pastén Salinas J. Forecasting models applied in solar photovoltaic and wind energy: a systematic mapping study. IEEE Access. 2024;12:151092–111. doi:10.1109/ACCESS.2024.3471073.
4. Mahdavi M, Jurado F, Schmitt K, Chamana M. Electricity generation from cow manure compared to wind and photovoltaic electric power considering load uncertainty and renewable generation variability. IEEE Trans Ind Appl. 2024;60(2):3543–53. doi:10.1109/TIA.2023.3330457.
5. Das A, Ni Z, Zhong X. Microgrid energy scheduling under uncertain extreme weather: adaptation from parallelized reinforcement learning agents. Int J Electr Power Energy Syst. 2023;152:109210. doi:10.1016/j.ijepes.2023.109210.
6. Chen ZC, Li CM. Energy emergency scheduling under extreme weather events: a novel emergency scheduling method based on the improved supernetwork. Energy. 2025;322:135491. doi:10.1016/j.energy.2025.135491.
7. Han S, He M, Zhao Z, Chen D, Xu B, Jurasz J, et al. Overcoming the uncertainty and volatility of wind power: day-ahead scheduling of hydro-wind hybrid power generation system by coordinating power regulation and frequency response flexibility. Appl Energy. 2023;333:120555. doi:10.1016/j.apenergy.2022.120555.
8. Song F, Cui J, Yu Y. Dynamic volatility spillover effects between wind and solar power generations: implications for hedging strategies and a sustainable power sector. Econ Model. 2022;116:106036. doi:10.1016/j.econmod.2022.106036.
9. He W, Xiong J, Chen W, Zhao W, Wang C. Optimal scheduling of combined heat and power based microgrid. In: 2020 IEEE/IAS Industrial and Commercial Power System Asia (I&CPS Asia); 2020 Jul 3–15; Weihai, China. p. 1411–5. doi:10.1109/icpsasia48933.2020.9208417.
10. Daneshvar M, Mohammadi-Ivatloo B, Zare K, Asadi S. Two-stage stochastic programming model for optimal scheduling of the wind-thermal-hydropower-pumped storage system considering the flexibility assessment. Energy. 2020;193:116657. doi:10.1016/j.energy.2019.116657.
11. Ma Y, Wang S, Yang H, Zhang D, Shen Y. Two-stage optimization model for day-ahead scheduling of electricity-heat microgrids with solid electric thermal storage considering heat flexibility. J Energy Storage. 2024;95:112329. doi:10.1016/j.est.2024.112329.
12. Chen H, Yang S, Chen J, Wang X, Li Y, Shui S, et al. Low-carbon environment-friendly economic optimal scheduling of multi-energy microgrid with integrated demand response considering waste heat utilization. J Clean Prod. 2024;450:141415. doi:10.1016/j.jclepro.2024.141415.
13. Tian X, Zha H, Tian Z, Lang G, Li L. Carbon emission reduction capability assessment based on synergistic optimization control of electric vehicle V2G and multiple types power supply. Energy Rep. 2024;11:1191–8. doi:10.1016/j.egyr.2024.01.003.
14. Zhu F, Li Y, Lu L, Wang H, Li L, Li K, et al. Life cycle optimization framework of charging-swapping integrated energy supply systems for multi-type vehicles. Appl Energy. 2023;351:121759. doi:10.1016/j.apenergy.2023.121759.
15. Fang C, Zhao X, Zhao Y, Tian Z, Yang Y, Li B. Electric vehicles participating in grid regulation interaction. In: Li H, Zhou Y, Feng D, Fang C, Wang N, editors. Optimization planning and operation of electric vehicle charging facilities. Amsterdam, The Netherlands: Elsevier; 2025. p. 175–217. doi:10.1016/b978-0-443-43952-0.00008-5.
16. Yu D, Guo Y, Zhu W. Optimal configuration of hydrogen storage capacity of hybrid microgrid considering peak regulation and frequency modulation requirements. Heliyon. 2024;10(17):e36674. doi:10.1016/j.heliyon.2024.e36674.
17. Sun B, Su X, Wang D, Zhang L, Liu Y, Yang Y, et al. Economic analysis of lithiumion batteries recycled from electric vehicles for secondary use in power load peak shaving in China. J Clean Prod. 2020;276(1):123327. doi:10.1016/j.jclepro.2020.123327.
18. Datta J, Das D. Energy management of multi-microgrids with renewables and electric vehicles considering price-elasticity based demand response: a bi-level hybrid optimization approach. Sustain Cities Soc. 2023;99(1):104908. doi:10.1016/j.scs.2023.104908.

19. Tan WY, Lei Y, Li J, Che Q, Liang W, Zhang Q. Research on the participation of electric vehicles in power grid dispatch considering dy-namic time-of-use electricity pricing. Renew Energy. 2020;38(11):1515–22. (In Chinese). doi:10.3969/j.issn.1671-5292.2020.11.015.
20. Dong Y, Wei AL, Zhu YS, Ku YH, Yang JL, Feng C. Research on dual-layer charging and discharging scheduling of electric vehicles considering user satisfaction. J Zhongyuan Univ Technol. 2020;31(3):63–70. (In Chinese). doi:10.3969/j.issn.1671-6906.2020.03.012.